Digital Filters

Review of Transforms

Definition	$H(e^{j\theta}) = \sum_{n=-\infty}^{\infty} h(n)\, e^{-jn\theta}$ $h(n) = \frac{1}{2\pi} \int_{-\pi}^{\pi} H(e^{jn\theta})\, e^{+j\theta}\, d\theta$
Periodicity	$H(e^{j\theta}) = H(e^{j(\theta+2k\pi)})$
Linearity	$a_1 h_1(n) + a_2 h_2(n)$ <--- DTFT ---> $a_1 H_1(e^{j\theta}) + a_2 H_2(e^{j\theta})$
Orthogonality	$\sum_{n=-\infty}^{\infty} h_1(n)\,[h_2(n)]^* = \frac{1}{2\pi} \int_{-\pi}^{\pi} H_1(e^{j\theta})\,[H_2(e^{j\theta})]^*\, d\theta$ $\sum_{n=-\infty}^{\infty} \lvert h_1(n)\rvert^2 = \frac{1}{2\pi} \int_{-\pi}^{\pi} \lvert H_1(e^{j\theta})\rvert^2\, d\theta$
Shifting	$h(n-k)$ <--- DTFT ---> $e^{-jk\theta}\, H(e^{j\theta})$ $e^{jn\varphi} h(n)$ <--- DTFT ---> $H(e^{j(\theta-\varphi)})$
Convolution	$h_1(n) * h_2(n)$ <--- DTFT ---> $H_1(e^{j\theta}) H_2(e^{j\theta})$ $h_1(n) h_2(n)$ <--- DTFT ---> $H_1(e^{j\theta}) \circledast H_2(e^{j\theta})$
Symmetry	$h(-n) = h(n)^*$ <--- DTFT ---> $\mathrm{Im}[H(e^{j\theta})] = 0$ $h(-n) = -h(n)^*$ <--- DTFT ---> $\mathrm{Re}[H(e^{j\theta})] = 0$ For a REAL-VALUED sequence : $H(e^{j\theta})^* = H(e^{-j\theta})$ $\lvert H(e^{j\theta})\rvert = \lvert H(e^{-j\theta})\rvert$ $\mathrm{Arg}\,[H(e^{j\theta})] = -\mathrm{Arg}\,[H(e^{-j\theta})]$ For an IMAGINARY-VALUED sequence : $-H(e^{j\theta})^* = H(e^{-j\theta})$

Table 1 DTFT

Definition	$H(k) = \sum_{n=0}^{N-1} h(n)\, e^{-j2\pi nk/N} = \sum_{n=0}^{N-1} h(n)\, W^{-nk}$ $h(n) = \frac{1}{N} \sum_{k=0}^{N-1} H(k) W^{nk}$
Periodicity	$H(k + N) = H(k)$
Linearity	$a_1 h_1(n) + a_2 h_2(n)$ <--- DFT: N ---> $a_1 H_1(k) + a_2 H_2(k)$
Orthogonality	$\sum_{n=0}^{N-1} h_1(n)\, [h_2(n)]^* = \frac{1}{N} \sum_{k=0}^{N-1} H_1(k)\, [H_2(k)]^*$ $\sum_{n=0}^{N-1} \lvert h_1(n)\rvert^2 = \frac{1}{N} \sum_{k=0}^{N-1} \lvert H_1(k)\rvert^2$
Shifting	$h(n - m)$ <--- DFT: N ---> $W^{-mk} H(k)$ $h(n)\, W^{nm}$ <--- DFT: N ---> $H(k - m)$
Convolution	$h_1(n) \circledast h_2(n)$ <--- DFT: N ---> $H_1(k) H_2(k)$ $h_1(n) h_2(n)$ <--- DFT: N ---> $H_1(k) \circledast H_2(k)$
Symmetry	$h(-n) = h(n)^*$ <--- DFT: N ---> Im[$H(k)$] = 0 $h(-n) = -h(n)^*$ <--- DFT: N ---> Re[$H(k)$] = 0 For a REAL-VALUED sequence : $H(k)^* = H(-k)$ $\lvert H(k \rvert = \lvert H(-k) \rvert$ Arg [$H(k)$] = -Arg [$H(-k)$] For an IMAGINARY-VALUED sequence : $-H(k)^* = H(-k)$ Note $h(-m) = h(N - m)$, $n < 0$ and $h(-m) = h(N - m)$, $k < 0$

Table 2 DFT

Definition	$H(z) = \sum_{n=-\infty}^{\infty} h(n)z^{-n}$		
Linearity	$\{h(n)\} = \{a\, h_1(n) + a\, h_2(n)\}$	<--->	$H(z)$
	$= a\, H_1(z) + b\, H_2(z)$		
Shifting	$\{h_d(n)\} = \{h(n - d)\}$	<--->	$H_d(z) = z^{-d} H(z)$
Convolution	$\{y(n)\} = \{h(n)\}*\{x(n)\}$	<--->	$Y(z) = X(z)H(z)$
Scaling	$\{a_n\, h(n)\}$	<--->	$H(z/a)$
Multiplication	$\{n^k\, h(n)\}$	<--->	$[-z \frac{d}{dz}]^k H(z)$

Table 3 *z*-transform

From Table 3, it can be seen that the output $y(n)$ at time n of a linear discrete time-invariant system is the convolution between the unit-sample response $h(n)$ and the input $x(n)$ and is given by

$$y(n) = \sum_{l=-\infty}^{\infty} h(l)x(n - l). \qquad (1)$$

Spectra Relationship between Fourier Transform and DTFT

If $H(e^{j\theta})$ is the DTFT of the sequence $\{t_0 h(nt_0)\}$ and $H(j\Omega)$ is the Fourier transform of $h_a(t)$, it can be shown that

$$H(e^{j\theta}) = \sum_{k=-\infty}^{\infty} H(j\Omega + jkw_0)\,|_{\Omega = w \text{ or } \Omega = \theta/t_0} \qquad (2)$$

where

$$w_0 t_0 = 2\pi \qquad (3)$$

$$\theta = w t_0 \qquad (4)$$

$$\Omega = w \qquad (5)$$

and t_0 is the sampling period. $H(e^{j\theta})$ is an aliased version of $H(j\Omega)$. If $H(j\Omega)$ is bandlimited to $-\Omega_m \le \Omega \le \Omega_m$, no aliasing would occur if $w_0 > 2\,\Omega_m$ ($f_0 > 2f_m$). f_0 is the Nyquist rate.

Relation between *z*-transform and DTFT

If $H(e^{j\theta})$ is the DTFT of the sequence $\{h(n)\}$ and $H(z)$ is the z-transform of $\{h(n)\}$, the connection between $H(e^{j\theta})$ and $H(z)$ is that the DTFT $H(e^{j\theta})$ is $H(z)$ restricted to the unit circle, i.e.,

$$H(e^{j\theta}) = H(z)|_{z = r\,e^{j\theta}} \qquad (6)$$

for $r = 1$. At a particular value of $\theta = \theta_0$, this corresponds to the intersecting point between the unit-circle and the line passing through the origin with an angle of θ_0 w.r.t. the real axis in the z-plane.

Introduction to Digital Filter

Digital filters are important class of linear time-invariant systems. The design of digital filters involves the following stages :

(1) The specification of the desired filter.
(2) The approximation of the specifications.
(3) The realisation of the filter.

When approximating a digital filter to meet a given specification, we should

(1) choose the type of filter;
(2) determine the filter coefficients; and
(3) verify the design w.r.t. the original specification.

In the previous section, we have seen the input/output relations of a linear discrete ime-invariant system. In the time-domain, the output $y(n)$ at time n is the convolution between the unit-sample response $h(n)$ and the input $x(n)$. The equation is given by

$$y(n) = \sum_{l=-\infty}^{\infty} h(l)x(n - l). \qquad (1)$$

The difference equation is

$$y(n) = \sum_{l=1}^{M} a_l \, y(n - l) + \sum_{l=-N_f}^{N_p} b_l \, x(n - l). \qquad (2)$$

In the z-transform domain, the system function $H(z)$ is given by

$$H(z) = \sum_{l=-N_f}^{N_p} b_l \, z^{-l} \, / \, [1 - \sum_{l=1}^{M} a_l \, z^{-l}] \qquad (3)$$

which can be factorised into the following product-of-sum form :

$$H(z) = Az^{N_f} \prod_{l=1}^{N_p + N_f} (1 - c_l \, z^{-1}) \, / \, [1 - \sum_{l=1}^{M} (1 - d_l \, z^{-1})). \qquad (4)$$

We can realise a digital filter from any one of these equations. When the filter structure is

determined from either the difference equation or the system function, the structure is known as the direct form 1. This is shown in Fig. 1.

Fig. 1

By considering $H(z) = H_1(z)H_2(z)$, where

$$H_1(z) = \frac{1}{1 + \sum_{l=1}^{M} a_l z^{-l}} \tag{5}$$

and

$$H_2(z) = \sum_{l=-N_f}^{N_p} b_l z^{-l}, \tag{6}$$

We can reduce the number of delay elements to the maximum of M or $N_p + N_f$. This memory-efficient structure is known as the direct form 2 (canonic form) and is shown in Fig. 2.

Fig. 2

Classification of Filters

Based on the filter structure, we can classify the filters into two categories. If the output is a function of the past outputs, the filter is referred to as a feed-back or a recursive filter. If the output is only a function of the input, the function is referred to as a feed-forward or a non-recursive filter. Alternatively, we can also classify the filters by the duration of their unit-sample response. If the filter produces a unit-sample response that has an infinite duration, the filter is referred to as an infinite-impulse response (IIR) filter. If the filter produces a unit-sample response that has a finite duration, the filter is referred to as a finite-impulse response (FIR) filter. The terms IIR and recursive are inter-changeable because some form of feedback path is required to achieve an infinite-duration unit-sample response. Similarly, the terms FIR and nonrecursive are interchangeable because a finite-duration unit-sample response can be obtained without any feedback structure.

Examples of Digital Filters

1. Comb Filter

$$H_C(z) = \frac{1-z^{-N}}{N} \qquad (7)$$

$H_C(z)$ is the system function of a comb filter. The filter structure is shown in Fig. 3.

Fig. 3

To obtain the frequency response of the filter, we simply substitute $z = e^{j\theta}$ into equation (7) and plot $|H(e^{j\theta})|$ or Arg $H(e^{j\theta})$ against θ. Thus,

$$H_C(e^{j\theta}) = \frac{1-e^{jN\theta}}{N}$$

$$H_C(e^{j\theta}) = (2j/N)\, e^{-jN\theta/2} \sin(N\theta/2) \qquad (8)$$

The corresponding magnitude response and the pole/zero pattern are shown in Figures 4 and 5, respectively.

Fig. 4

Fig.5

2. Resonator

$$H_R(z) = \frac{G_R}{1-z^{-1}} \qquad (9)$$

$H_R(z)$ is the system function of a resonator. The filter structure is shown in Fig. 6.

Fig. 6

The resonator generates a pole at $z = 1$ and a zero at $z = 0$. Since the pole lies on the unit circle, the filter is unstable. When this resonator is cascaded with the comb filter, the zero of the comb filter located at $z = 1$ cancels the resonator pole, making the entire system to become stable.

$$H_C(e^{j\theta})\, H_R(e^{j\theta}) = \frac{G_R}{N} \frac{1-e^{jN\theta}}{1-e^{j\theta}}$$

$$H_C(e^{j\theta})\, H_R(e^{j\theta}) = \frac{G_R}{N}\, e^{-j(N-1)\theta/2} \sin(N\theta/2)/\sin(\theta/2) \qquad (10)$$

Fig. 7 shows the magnitude response.

Fig. 7

Practical Desired Filter Specifications

In practice, the desired magnitude response $|H(e^{j\theta})|$ is usually specified and the phase response is left unspecified. The magnitude response specifications will consist of passband and stopband regions. Fig. 8 shows the regions for lowpass, highpass, bandpass and bandstop filters.

Fig. 8

Design of Digital Filters

1. IIR Filter Design

Infinite-impulse response digital filters are commonly used to replace existing analog filters. Readers should refer to the appendix section for the design of analog filters. In this section, we shall discuss three commonly employed methods for the design of IIR filters.

1.1 Impulse-Invariant Method

IIR digital filters have system functions of the form

$$H(z) = \sum_{l=-N_f}^{N_p} b_l\, z^{-l} \,/\, [1 - \sum_{l=1}^{M} a_l\, z^{-l}]. \qquad (11)$$

The impulse-invariant method produces an IIR digital filter whose unit-sample response is equal to the scaled, sampled version of the analog filter impulse response $h_a(t)$, i.e.,

$$t_0 h(nt_0) = h_a(t)\,|_{t = nt_0} \qquad (12)$$

where t_0 is the sampling period and $h(nt_0)$ is the digital filter unit-sample response at time $t = nt_0$. t_0 is included in equation (12) to ensure that the digital filter gain $|H(e^{j\theta})|$ is independent of the sampling period. Some people may prefer to design a digital filter such that $h(nt_0) = h_a(t)\,|_{t = nt_0}$. In this case, the following results should be adjusted by the scaling factor t_0.

If $|H(e^{j\theta})|$ is the DTFT of the sequence $\{t_0 h(nt_0)\}$ and $H(j\Omega)$ is the Fourier transform of $h_a(t)$, it can be shown that

$$H(e^{j\theta}) = \sum_{k=-\infty}^{\infty} H(j\Omega + jkw_0)\,|_{\Omega = w \text{ or } \Omega = \theta/t_0} \qquad (13)$$

for $w_0 t_0 = 2\pi$ and $\theta = wt_0$. Equation (13) indicates that $H(e^{j\theta})$ is an aliased version of $H(j\Omega)$. If $H(j\Omega)$ is bandlimited to $-\Omega_m \leq \Omega \leq \Omega_m$, no aliasing would occur if $w_0 \geq 2\Omega_m$ ($f_0 > 2f_m$). However, practical filters are not truely bandlimited and some degree of aliasing will always occur. Therefore, the impulse-invariant method should be restricted to narrow-band filters with sharp cut-off at $w_0/2$ (the foldover frequency point).

The representation of the aliasing that occurs in the impulse-invariant method can be illustrated by the mapping between points in the *s*-plane and the *z*-plane. Since

$$w_0 t_0 = 2\pi \qquad (14)$$

$$\theta = wt_0 \qquad (15)$$

$$\Omega = w \qquad (16)$$

$$z = 1\, e^{j\theta} \qquad (17)$$

$$s = \sigma + j\,\Omega\,, \qquad (18)$$

then

$$z = e^{st_0}\,. \qquad (19)$$

Strips of width $\Omega = 2\pi/t_0$ in the *s*-plane map into the entire *z*-plane as shown in Fig. 9.

Fig. 9

Different points on the *s*-plane (e.g., $s = j\pi/t_0$ and $s = j3\pi/t_0$) may map onto the same point in the *z*-plane ($z = -1$).

Example

Calculate the digital filter system function $H(z)$ corresponding to the analog filter response of $H(s)$ =2s/(s2+3s+2).

$$H(s) = 2s/(s^2 + 3s + 2)$$

$H(s) = 2s/[(s + 2)(s + 1)]$

$H(s) = 4(s + 2)^{-1} - 2/(s + 1)^{-1}$

$h_a(t) = \text{LT}^{-1} H(s)$

$h_a(t) = 4e^{-2t} - 2e^{-1t}$

$h(nt_0) = h_a(t)\,|_{t = nt_0},\ n \geq 0$

$h(nt_0) = 4e^{-2nt_0} - 2e^{-1nt_0}$

$t_0 h(nt_0) = t_0 4e^{-2nt_0} - t_0 2e^{-1nt_0}$

and $H(z) = \sum_{n=0}^{\infty} t_0 h(nt_0) z^{-n}$

$H(z) = \sum_{n=0}^{\infty} t_0 4e^{-2nt_0} z^{-n} - \sum_{n=0}^{\infty} t_0 2e^{-1nt_0} z^{-n}$

$H(z) = \sum_{n=0}^{\infty} t_0 4(e^{-2nt_0} z^{-1})^n - \sum_{n=0}^{\infty} t_0 2(e^{-1nt_0} z^{-1})^n$

Since an infinite geometric series $\sum_{n=0}^{\infty} c_n$ converges to $(1 - c)^{-1}$ for $|c| < 1$, the z-transform $H(z)$ becomes

$$H(z) = \frac{t_0 4}{1 - e^{-2t_0} z^{-1}} - \frac{t_0 2}{1 - e^{-1t_0} z^{-1}}$$

Fig. 9.1

Summary

1. Given $H(s)$.
2. Find the partial fraction form of $H(s)$.
3. Replace $H(s)$ by $H(z)$.
4. Plot $H(j\Omega)$ Vs Ω and $H(e^{j\theta})$ Vs w.

1.2 Bilinear Transformation

The bilinear transformation provides a non-linear one-to-one mapping of the point on the $j\Omega$ axis in the s-plane to the points on the unit circle in the z-plane. A simple bilinear transformation is

$$s = (z - 1)/(z + 1) \tag{20}$$

or

$$z = (1 + s)/(1 - s). \tag{21}$$

By setting $z = e^{j\theta} = e^{jwt0}$ in equation (20), the relationship between Ω in the s-plane and w in the z-plane is found.

$$\Omega = \tan \theta/2 \tag{22}$$

or

$$\theta = 2 \tan^{-1} \Omega. \tag{23}$$

Equation (21) and (23) are summarised in Figures (10) and (11), respectively.

Fig. 10

Fig. 11

It can be seen that a one-to-one mapping avoids the problem of aliasing. The price paid for this is the non-linear compression of frequency axis as shown in Figure 11. Ω is called a frequency warping. This compression can be compensated by pre-warping the frequencies (usually the passband frequency Ω_p and the stopband frequency Ω_s) of the analog filter using $\Omega^* = \tan \Omega t_0/2$. When the bilinear transformation is applied, $|H(e^{j\theta})|$ will meet the original specifications. Figure 12 shows the frequency prewarping procedure.

Fig. 12

Given $H(j\Omega)$ (the original specifications), the resulting digital filter magnitude response $|H(e^{j\theta})|$ will meet the original specifications (i.e., $w_p = \Omega_p$ and $w_s = \Omega_s$)

providing we pre-warp $H(j\Omega)$ to $H(j\Omega^*)$ before the bilinear transformation.

Example

Calculate the digital filter system function $H(z)$ corresponding to the analog filter response of $H(s) = 1/(s + \Omega_c)$ using bilinear transformation. The sampling period t_0 is set at π seconds and $\Omega_c = 0.5$ radians/second.

The prewarping frequency $\Omega^* = \tan \Omega_c t_0/2$. Therefore, $\Omega_c^* = 1$ radian/sec. and

$$H(j\Omega^*) = 1/(s + \Omega_c^*)$$
$$H(j\Omega^*) = 1/(s + 1).$$

Substitute $s = (z - 1)/(z + 1)$ into the above equation. Thus

$$H(z) = (1 + z^{-1})/2.$$

Summary

1. Given $H(s = j\Omega)$ and t_0.
2. Find $H(s = j\Omega^*)$ by prewarping frequencies using $\Omega^* = \tan (\Omega t_0/2)$.
3. Find $H(z)$ by bilinear transformation.
4. Plot $H(j\Omega)$ Vs Ω and $H(e^{j\theta})$ Vs w.

Although the bilinear transformation eliminates the effect of aliasing effect, the mapping function also manifests itself as a warping of the phase response. Suppose we have Arg $H(s = j\Omega) = kj\Omega$, the phase of the digital filter can be found by substituting equation (22) into $kj\Omega$. Hence, the phase of the digital filter is Arg $H(z = e^{j\theta}) = kj \tan (\theta/2)$. This is shown in Figure 13.

Fig. 13

From Figure 13, it can be seen that we cannot get a linear phase digital filter by applying the bilinear transformation to a linear phase analog filter.

Comparsion

Impulse-invariant method	Bilinear transformation

1.	$z = e^{st_0}$, $s = (\log_e z)/t_0$, $\Omega = \theta/t_0$	$z = (1 + s)/(1 - s)$, $s = (z - 1)/(z + 1)$, $\Omega = \tan(\theta/2)$
2.	System stability is maintained.	System stability is maintained.
3.	No phase distortion but scaled.	Phase distortion (i.e., warping)
4.	Aliasing effect.	No aliasing effect.
5.	For and filter design.	For all types of filter design.
6.	$\lvert H(j\Omega)\rvert \simeq \lvert H(e^{j\theta})\rvert$ $t_0 h(nt_0) = h(t)\lvert_{t = nt_0}$ This error is caused by the aliasing.	$\lvert H(j\Omega)\rvert = \lvert H(e^{j\theta})\rvert$
7.	Application is restricted to $\lesssim$ and $\gtrsim$ filters with sharp cut-off to avoid severe aliasing effect.	No restriction.

Table 1

1.3 Matched *z*-transformation

The matched *z*-transformation is similar to the impulse-invariant method. In this case, the analog filter $H(s)$ is transformed by replacing both poles and zeros by :

i-th zero : $s + q_i$ --> $1 - e^{q_i t_0} z^{-1}$

i-th pole : $s + p_i$ --> $1 - e^{p_i t_0} z^{-1}$

Example

$H(s) = (s + 1)/(s + 2)$

$H(z) = (1 - e^{t_0} z^{-1})/(1 - e^{2t_0} z^{-1})$.

This mapping method can sometimes transform high-frequency zeros to low-frequency zeros in the digital filter's response. Thus, it is not often used.

Frequency Transformations

Once we have designed the digital lowpass filter, we can employ frequency transformations to produce with different cut-off frequency values, highpass filters, bandpass filters, or bandstop filters. These transformations are applied by replacing each z-1 in the designed lowpass filter with the entry in Table 2.

Lowpass	$\frac{(z^{-1}-\alpha)}{(1-\alpha z^{-1})}$	$\alpha = \frac{\sin[(\theta_{p1}-\theta_{p2})/2]}{\sin[(\theta_{p1}+\theta_{p2})/2]}$
Highpass	$-\frac{(z^{-1}-\alpha)}{(1-\alpha z^{-1})}$	$\alpha = -\frac{\cos[(\theta_{p1}+\theta_{p2})/2]}{\cos[(\theta_{p1}-\theta_{p2})/2]}$
Bandpass	$-\frac{z^{-2}-\frac{2\alpha k}{k+1}z^{-1}+\frac{k-1}{k+1}}{\frac{k-1}{k+1}z^{-2}-\frac{2\alpha k}{k+1}z^{-1}+1}$	$\alpha = \frac{\cos[(\theta_{pu2}+\theta_{pl2})/2]}{\cos[(\theta_{pu1}-\theta_{pl2})/2]}$
Bandstop	$-\frac{z^{-2}-\frac{2\alpha m}{1+m}z^{-1}+\frac{1-m}{1+m}}{\frac{1-m}{1+m}z^{-2}-\frac{2\alpha}{1+m}z^{-1}+1}$	$\alpha = \frac{\cos[(\theta_{pu1}+\theta_{pl2})/2]}{\cos[(\theta_{pu1}-\theta_{pl2})/2]}$

$k = \cot[(\theta_{pu2} - \theta_{pl2})/2] \tan(\theta_{p1}/2)$

$m = \tan[(\theta_{pu2} - \theta_{pl2})/2] \tan(\theta_{p2}/2)$

θ_{p1} = original passband frequency specification

θ_{p2} = transformed passband frequency specification

θ_{pu2} = transformed upper passband frequency specification

θ_{pl2} = transformed lower passband frequency specification

Table 2

Example

Transform the Chebyshev lowpass digital filter $H_1(z)$ into a Chebyshev lowpass digital filter $H_2(z)$ where

$$H_1(z) = \frac{4.29(10^{-3})(1+z^{-1})(1+z^{-1})(1+z^{-1})}{(1-0.801z^{-1})[1-(0.819+j\ 0.373)z^{-1})][1-(0.819-j\ 0.373)z^{-1})]},$$

$\theta_{p1} = 0.1404\pi$ and $\theta_{p2} = 0.2808\pi$.

1. Find α :

$$\alpha = \frac{\sin[\theta_{p1} - \theta_{p2}]/2}{\sin[\theta_{p1} + \theta_{p2}]/2}$$

α = -0.356

2. Zero transformations :

$$(1 - c_i z^{-1}) \text{ ---> } 1 - c_i \frac{z^{-1} - \alpha}{1 - \alpha z^{-1}} = (1 - c_i \alpha) \frac{1 - [(\alpha + c_i)/(1 + \alpha c_i)]z^{-1}}{1 - \alpha z^{-1}}$$

A zero at $z = c_i$ is therefore transformed into a zero at $z = (\alpha + c_i)/(1 + c_i \alpha)$ and the corresponding pole at $z = 0$ is transformed into a pole at $z = \alpha$. Thus,

c_i	$(\alpha + c_i) / (1 + c_i \alpha)$
-1	1

and $(1 + c_i \alpha) = 1.356$.

3. Pole transformations :

$$\frac{1}{1 - d_i z^{-1}} \text{ ---> } [1 - d_i (\frac{z^{-1} - \alpha}{1 - \alpha z^{-1}})]^{-1} = \frac{1 - \alpha z^{-1}}{(1 + d_i \alpha)\{1 - [(\alpha + d_i)/(1 + d_i \alpha)]z^{-1}\}}$$

A pole at $z = d_i$ is therefore transformed into a pole at $z = (\alpha + d_i)/(1 + d_i \alpha)$ and the corresponding zero at $z = 0$ is transformed into a zero at $z = \alpha$. Thus,

d_i	$(\alpha + d_i) / (1 + d_i \alpha)$

0.801	0.622
0.819 + j0.373	0.535 +j0.627
0.819 - j0.373	0.535 -j0.627

---

and $(1 + d_i\ \alpha) = 0.715$ for $d_i = 0.801$,

$(1 + d_i\ \alpha) = 0.71+0.133j$ for $d_i = 0.819 + j0.373$,

$(1 + d_i\ \alpha) = 0.71-0.133j$ for $d_i = 0.819 - j0.373$.

4. Find $H_2(z)$:

$$H_2(z) = \frac{A\ (1+c_i\ \alpha\ )(1+z^{-1})(1+z^{-1})(1+z^{-1})}{0.715(0.819+j\ 0.373)(0.819-j\ 0.373)B}$$

where

$A = 4.29(10^{-3})$

$B = (1 + 0.622z^{-1})(0.535 + j0.627)(0.535 - j0.627)$.

Thus,

$$H_2(z) = \frac{0.029(1+z^{-1})(1+z^{-1})(1+z^{-1})}{(1+0.622z^{-1})(0.535+j\ 0.627)(0.535-j\ 0.627)}$$

5. Pole/zero pattern and magnitude response curves :

Fig. 13.1

2. FIR Filter Design

In contrast to IIR filters, the finite-impulse response (FIR) filter has a finite duration unit-sample response. The system function of an FIR filter can be written as

$$H(z) = \sum_{l=-N_f}^{N_p} b_l z^{-l} . \qquad (24)$$

Several design methods are described here. If the unit-sample response $\{h_D(n)\}$ is given and has a finite duration, the FIR filter can be implementeddirectly from the coefficients b_l where

$$h_D(n) = b_{l=n} \qquad (25)$$

for $-N_f \le n,\ l \le N_p$. This is shown in Fig. 14.

Fig. 14

If $\{h_D(n)\}$ is given and has an infinite duration, the windowing method is used for designing FIR filters. If $\{h_D(n)\}$ is not given and the desired magnitude response $|H_D(e^{j\theta})|$ is given, the DFT/windowing method is used for designing FIR filters. Alternatively, the frequency sampling method can be used.

2.1 Windowing Method

Our goal here is to choose an appropriate window to give a FIR digital filter with unit-sample response $\{h_N(n)\}$ of length N which is close to $H_D(e^{j\theta})$, where $H_D(e^{j\theta})$ is the discrete-time Fourier transform of the infinite-duration desired unit-sample response $\{h_D(n)\}$. We will restrict the design to linear phase filters.

The steps in performing windowing FIR digital filter design are :

1. Multiply $\{h_D(n)\}$ with an N-point window to obtain $\{h_N(n)\}$.
2. Compute the DTFT of $\{h_N(n)\}$.
3. Compare $|H_N(e^{j\theta})|$ with the desired $|H_D(e^{j\theta})|$.
4. Repeat steps 1-3 with another window if $|H_N(e^{j\theta})|$ is not close enough to $|H_N(e^{j\theta})|$.

Several common window sequences are :

1. the rectangular window,
2. the triangular (Bartlett) window,
3. the raised-cosine (Hanning) window,
4. the Hamming window, and
5. the Blackman window.

2.1.1 The Rectangular Window

The rectangular window sequence is defined by

$$w(n) = 1 \text{ for } -(N-1)/2 \le n \le (N-1)/2$$
$$w(n) = 0 \text{ otherwise.} \qquad (26)$$

The DTFT of the rectangular window is

$$W(e^{j\theta}) = \sum_{n=-(N-1)/2}^{(N-1)/2} e^{-j\theta n} \qquad (27)$$

$$W(e^{j\theta}) = e^{j\theta(N-1)/2} \sum_{n=0}^{N-1} e^{-j\theta n} \qquad (28)$$

Since $\sum_{n=0}^{N-1} c^n = (1 - c^N)/(1 - c)$, equation (28) can be expressed as

$$W(e^{j\theta}) = e^{j\theta(N-1)/2} \frac{1-e^{-j\theta N}}{1-e^{-j\theta}}$$

$$W(e^{j\theta}) = \sin(N\theta)/\sin(\theta/2) \qquad (29)$$

Example

Design a FIR filter of length $N = 15$ that approximates an ideal low-pass filter with $\theta_c = \pi/4$. The desired response is

$$H_D(e^{j\theta}) = 1 \quad \text{for } -\theta_c \le \theta \le \theta_c$$
$$= 0 \quad \text{for } -\pi \le \theta < -\theta_c \text{ and } \theta_c < \theta < \pi. \qquad (30)$$

The unit-sample response of the desired low-pass filter is

$$h_D(n) = \frac{1}{2\pi} \int_{-\pi}^{\pi} H(e^{j\theta})\, e^{j\theta n}\, d\theta$$

$$h_D(n) = \sin(\theta_c n)/\pi n \quad \text{for all } n. \qquad (31)$$

$\{h_D(n)\}$ is approximated by $\{h_N(n)\}$ of length N by multiplying $h_D(n)$ with the rectangular window, or

$$\{h_N(n)\} = \{w(n)\, h_D(n)\}$$

$$\{h_N(n)\} = \{\sin(\theta_c n)/\pi n\} \quad \text{for } -(N-1)/2 \le n \le (N-1)/2 \qquad (32)$$

The corresponding magnitude response and the unit-sample response curves are shown in Fig. 15.

Fig. 15

The shape of $H_N(e^{j\theta})$ is obtained by convolving $H_D(e^{j\theta})$ with $W(e^{j\theta})$. From the above example, several observations can be made.

1. The mainlobe width is equal to $2a$ where $a = 2\pi/N$.
2. The sidelobe is -13 dB relative to the maximum value at $\theta = 0$.
3. The sharp transition in the desired response $H_D(e^{j\theta})$ at θ_c has been converted into a gradual transition.
4. A series of overshoots and undershoots occur in the passband.
5. A series of leakage occurs in the stopband.

In general, the width in the transition region of $H_N(e^{j\theta})$ is related to $2a$ and the width can be reduced by increasing N. The effect of the sidelobes in $W(e^{j\theta})$ causes $H_N(e^{j\theta})$ to have overshoots and undershoots in the passband, and leakage in the stopband. These ripples remain almost constant no matter how large the value of N is. This is known as the Gibbs phenomenon. The sidelobes in $W(e^{j\theta})$ represent the high-frequency components in the window sequence. These components are due to the sharp transitions from 0 --> 1 or 1 --> 0 at the edges of the rectangular window sequence. If we can replace the rectangular window sequence by a sequence with gradual transitions, the sidelobe levels in $W(e^{j\theta})$ can be reduced which, in turn, also reduces the variations in the passband and the sidelobe levels in the stopband of $H_N(e^{j\theta})$. Some commonly used windows are given in Table 3 and the effects of using these windows are shown in Fig. 16.

Window Type	$w(n)$ for $-(N-1)/2 \leq n \leq (N-1)/2$
Rectangular	$w(n) = 1$ for n, $= 0$ otherwise
Triangular	$w(n) = 1 - [\, 2\,\lvert n\rvert / (N-1)\,]$
Raised-Cosine (Hanning)	$w(n) = 0.5+0.5 \cos [2\pi n/(N-1)]$ for n, $= 0$ otherwise
Hamming	$w(n) = 0.54 + 0.54 \cos[2\pi n/(N-1)]$ for n, $= 0$ otherwise

Blackman	$w(n) = 0.42 + 0.5\cos[2\pi n/(N - 1)] + 0.08\cos[4\pi n/(N - 1)]$ for n, = 0 otherwise

Window Type	First Sidelobe Peak Amp. (dB)	Mainlobe width
Rectangular	-13	$4\pi/N$
Triangular	-25	$8\pi/N$
Hanning	-31	$8\pi/N$
Hamming	-41	$8\pi/N$
Blackman	-57	$12\pi/N$

Table 3

Fig. 16

Regarding the choice of a particular window for the filter design, the important parameter is not the shape $W(e^{j\theta})$ but rather its effect on $H_N(e^{j\theta})$. Table 3 shows that there is a tradeoff between the mainlobe width and the first sidelobe level. Referring to Figure 16, the stopband magnitude response of the windows and the corresponding final filters are summarised in Tables 4 and 5.

Window	Stopband properties
▭	Attenuation increases as θ --> π.
△	As above. More attenuation than ▭.
⩚	As above. More attenuation than △.
	Attenuation remains almost constant. Most sidelobes lie between ▭ and △ sidelobes.

	Attenuation increases asθ --> π. More attenuation than  .

Table 4

$\lvert H_N(e^{j\theta}) \rvert$	Stopband properties
with	See Table 4.
with	See Table 4. Smoother attenuation.
with 	See Table 4.
with 	See Table 4.
with 	See Table 4. The first sidelobe peak is at θ > π/2.

Table 5

2.2 DFT/Windowing Method

The DFT/windowing method involves two stages. Given a digital filter specification $|H(e^{j\theta})|$ and phase response, our first goal is to obtain the desired magnitude response $|H_D(e^{j\theta})|$ and to find a finite-duration approximation, denoted by $\{h_d(n)\}$, to the desired unit-sample response $\{h_D(n)\}$. Having determined $\{h_d(n)\}$, our second goal is to reduce the overshoots and leakage effects in $|H_d(e^{j\theta})|$ caused by applying the DFT method in the first place. These effects can be reduced by the windowing method. The windowing method gives a finite-duration unit-sample response $\{h_N(n)\}$ which is shorter than $\{h_d(n)\}$ and meets our desired specifications. The design procedure is shown in Figure 17 and we will consider $h_d(n) = h_D(n)$ for the N_d points over which $\{h_d(n)\}$ is defined.

Fig. 17

To illustrate the DFT/windowing method, let us restrict to the filter whose phase response

is linear. An example is given below.

Example

Design a zero-phase low-pass digital filter whose specification is shown in Figure 18.

Fig. 18

(a) Sketch the desired magnitude response $|H_D(e^{j\theta})|$

Since the resulting magnitude response exhibits a reduction in the passband when applying the windowing method, $|H_D(e^{j\theta})|$ should have its 3-dB cut-off point extended into the transition region. A good guess for this extension is equal to 30% of the transition region. This is shown in Figure 19.

Fig. 19

(b) Choose the value N_d, the length of $\{h_d(n)\}$

The inverse DFT of $\{H_D(k)\}$ (the sample version of $H_D(e^{j\theta})$) produces a periodic sequence $\{h_d(n)\}$ where $\{h_d(n)\}$ is the periodic extension of $\{h_d(n)\}$. If $\{h_D(n)\}$ has an infinite duration, $\{h_d(n)\}$ will not equal to it. Some degree of time-aliasing will occur. We should therefore consider large value of N_d such that $h_d(n) = h_D(n)$ over which $\{h_d(n)\}$ is defined. The time-aliasing can then be minimised. $N_d = 128$ is a good choice and $N_d >> N$ where N is the length of $\{h_N(n)\}$. For our example, we set $N_d = 16$ to ease the analysis. The results are shown in Figure 20.

Fig. 20

Form Figure 20, it can be seen that

$$H_D(k) = H_D(e^{j\theta})|_{\theta = 2\pi k/N_d} \qquad (33)$$

for $0 \le k \le N_d - 1$. In general, $\{H_D(k)\}$ is a complex-valued discrete N_d-periodic sequence and it can be expressed as

$$H_D(k) = H_R(k) + jH_I(k) \qquad (34)$$

where

$$H_R(k) = |H_D(k)| \cos [\text{Arg } H_D(k)] \tag{35}$$

and

$$H_I(k) = |H_D(k)| \sin [\text{Arg } H_D(k)]. \tag{36}$$

For our example, $[\text{Arg } H_D(k)] = 0$ for all k. Thus $H_R(k) = |H_D(k)| = 1$ and $H_I(k) = 0$. The inverse DFT of $\{H_R(k)\}$ is an N_d-periodic sequence $\{\tilde{h}_d(n)\}$ and $\{\tilde{h}_d(n)\}$ is the periodic extension of $\{h_d(n)\}$. The N_d-point sequence $\{h_d(n)\}$ is extracted from the inverse DFT sequence $\{\tilde{h}_d(n)\}$ where

$$\tilde{h}_d(n) = \frac{1}{N} \sum_{k=0}^{N_d - 1} H_D(k)\, e^{j2\pi nk/N_d} \tag{37}$$

for $0 \le n \le N_d - 1$.

(c) Compute $H_d(e^{j\theta})$, the DTFT of $\{h_d(n)\}$

The DTFT of $\{h_d(n)\}$ is

$$H_d(e^{j\theta}) = \sum_{n=(-N_d/2)+1}^{N_d/2} h_d(n)\, e^{j\theta n} \tag{38}$$

For our example, the time and frequency responses are shown in Figure 21. In general, the value of $H_d(e^{j\theta})$ at the sampling instants equals $H_D(k)$, i.e.,

$$H_D(k) = H_d(e^{j\theta})\big|_{\theta = 2\pi k/N_d} \tag{39}$$

Fig. 21

(d) Determine the N-point unit-sample response $\{h_N(n)\}$

To reduce the overshoots and leakage effects of $H_d(e^{j\theta})$, the windowing method can be applied to $\{h_d(n)\}$. $\{h_d(n)\}$ is multiplied by an N-point window to obtain $\{h_N(n)\}$ for $N << N_d$. $N = N_d/2$ is a good choice.

(e) Compute $H_{N_d}(e^{j\theta})$ and $H_{N_d}(k)$

Compute the N_d -point DFT of $\{h_N(n)\}$ to obtain $\{H_{N_d}(k)\}$ or the DTFT of $\{h_N(n)\}$ to obtain $H_{N_d}(e^{j\theta})$ for $0 \leq \theta \leq 2\pi$. If specification is met, we try to employ a smaller value of N. If specification is not met, we try to increase the value of N.

2.3 Frequency-Sampling Method

This method is similar to the DFT/windowing method. The difference is that we do not compute the inverse DFT to determine the unit-sample response $\{h_d(n)\}$ of the FIR filter. Given a desired magnitude response specification $|H_D(k)|$ of a digital filter, our goal is to find a system function $H_d(z)$ such that $H_D(k)$ is a sample version of $H_d(z)|_{z = e^{j2\pi k/N_d}}$. The design procedure is shown in Figure 22.

Fig. 22

If $\{h_d(n)\}$ is the unit-sample response sequence of an FIR filter, then the N_d-point DFT is

$$H_D(n) = \sum_{n=0}^{N_d - 1} h_d(n)\, e^{-j2\pi nk/N_d}. \qquad (40)$$

From our discussion of the z-transform, the connection between $H_d(e^{j\theta})$ and $H_d(z)$ is that the DTFT $H_d(e^{j\theta})$ is the $H_d(z)$ restricted to the unit circle in the z-plane, where

$$H_d(z) = \sum_{n=0}^{N_d - 1} h_d(n)\, z^{-n}. \qquad (41)$$

Since The IDTFT of $\{H_d(k)\}$ is

$$h_d(n) = \frac{1}{N_d} \sum_{k=0}^{N_d - 1} H_D(k)\, e^{j2\pi nk/N_d}. \qquad (42)$$

for n = 0, 1, ..., N_d - 1, equation (41) becomes

$$H_d(z) = \frac{1}{N_d} \sum_{n=0}^{N_d-1} \sum_{k=0}^{N_d-1} H_D(k)\, e^{j2\pi nk/N_d}.\, z^{-n}$$

$$H_d(z) = \frac{1}{N_d} \sum_{k=0}^{N_d-1} H_D(k) \left[\sum_{n=0}^{N_d-1} e^{j2\pi nk/N_d} z^{-n} \right]$$

$$H_d(z) = \frac{1}{N_d} H_D(k) \left[\frac{1-z^{-N_d}}{1-e^{j\,2\pi nk\,/N_d} z^{-1}} \right] \qquad (43)$$

and

$$H_d(e^{j\theta}) = H_d(z)|_{z = e^{j\theta}} \qquad (44)$$

Since

$$H_D(k) = H_D(e^{j\theta})|_{\theta = 2\pi k/N_d} \qquad (45)$$

for $0 \leq k \leq N_d - 1$, the FIR filter whose magnitude response $|H_d(e^{j\theta})|$ exactly matches the desired magnitude response $|H_D(k)|$ at the sampling points.

Example

Design a FIR filter based on an 8-point DFT $\{H_D(k)\} = \{1, 1, 0, 0, 0, 0, 0, 1\}$ using frequency sampling method.

From equation (43),

$$H_d(z) = \frac{1}{8} \sum_{k=0}^{7} \frac{1-z^{-8}}{1-e^{j\pi k\,/4} z^{-1}}$$

$$H_d(z) = \frac{1-z^{-8}}{8} \left[\frac{1}{1-z^{-1}} + \frac{1}{1-z^{-1}(\cos \pi/4 + j\, \sin \pi/4)} + \frac{1}{1-z^{-1}(\cos 7\pi/4 + j\, \sin 7\pi/4)} \right]$$

$$H_d(z) = \frac{1-z^{-8}}{8} \left[\frac{1}{1-z^{-1}} + \frac{1}{1-z^{-1}(1/\sqrt{2} + j\, 1/\sqrt{2})} + \frac{1}{1-z^{-1}(1/\sqrt{2} - j\, 1/\sqrt{2})} \right]$$

$$H_d(z) = \frac{1-z^{-8}}{8} \left[\frac{1}{1-z^{-1}} + \frac{2-\sqrt{2}z^{-1}}{1-\sqrt{2}z^{-1}+z^{-2}} \right]$$

Figures 23 and 24 give the filter implementation and the response curves, respectively.

Fig. 23

Fig. 24

Excessive overshoots and leakage effects can then be reduced by the windowing method.

Summary

1. Windowing method

1.1 Given $\{h_D(n)\}$ of infinite duration, find $\{h_N(n)\}$ of length N.

1.2 The important parameter is the effect of $W(e^{j\theta})$ on $|H_N(e^{j\theta})|$.

1.3 Gibbs phenomenon is observed.

1.4 A trade-off between the main-lobe width and the first side-lobe level of $W(e^{j\theta})$.

2. DFT/Windowing method

2.1 Given $|H_D(e^{j\theta})|$ and Arg $H_D(e^{j\theta})$, find $\{h_d(n)\}$ of length N_d and $\{h_N(n)\}$ of length N where $N << N_d$.

2.2 N_d = 128 is usually a good choice.

2.3 $N = N_d/2$ is also a good starting value.

3. Frequency-sampling method

3.1 Given $|H_D(k)|$, find $H_d(z)$ such that $H_D(k)$ is a sample version of $H_d(z)|_{z = e^{j2\pi k/N_d}}$.

3.2 Excessive overshoots and leakage effects without the application of the windowing.

3.3 The method really shines when $|H_D(k)|$ has a specific shape.

Comparison Between IIR and FIR Filters

The choice of whether to use FIR or IIR filters depends on the application and the hardware complexity. In general, FIR (non-recursive) filters are always stable and they are ideally suited for use in time-varying applications. They are also suited to multi-rate DSP problems where data sequences are sampled at different rates. Linear phase response is easily obtainable with FIR filters. On the other hand, IIR (recursive) filters have simple design methods. IIR filters can produce much sharper transitions in

amplitude response with fewer delay elements than FIR filters. So, the choice is not clear-cut and one must evaluate several factors before making a decision.

References

[1] Kuc, R., 'Introduction to Digital Signal Processing', McGraw-Hill, 1982.

[2] Robert, R. A. and Mullis, C. T., 'Digital Signal Processing', Addison- Wesley, 1987.

[3] Oppenheim, A. V. and Schafer, R. W., 'Discrete-Time Signal Processing', Prentice Hall, 1989.

[4] Blinchikoff, H. J. and Zverev, A. I., 'Filtering in the Time and Frequency Domains', J Wiley, 1976.

[5] Hamming, R. W., 'Digital Filters', 2/e, Prentice-Hall, 1983.

[6] Lam, H. Y.-F., 'Analog and Digital filters', Prentice-Hall, 1979.

[7] Van Valkenburg, M. E., 'Analog Filter Design', Holt, Rinehart and Winstion Pubs., 1982.

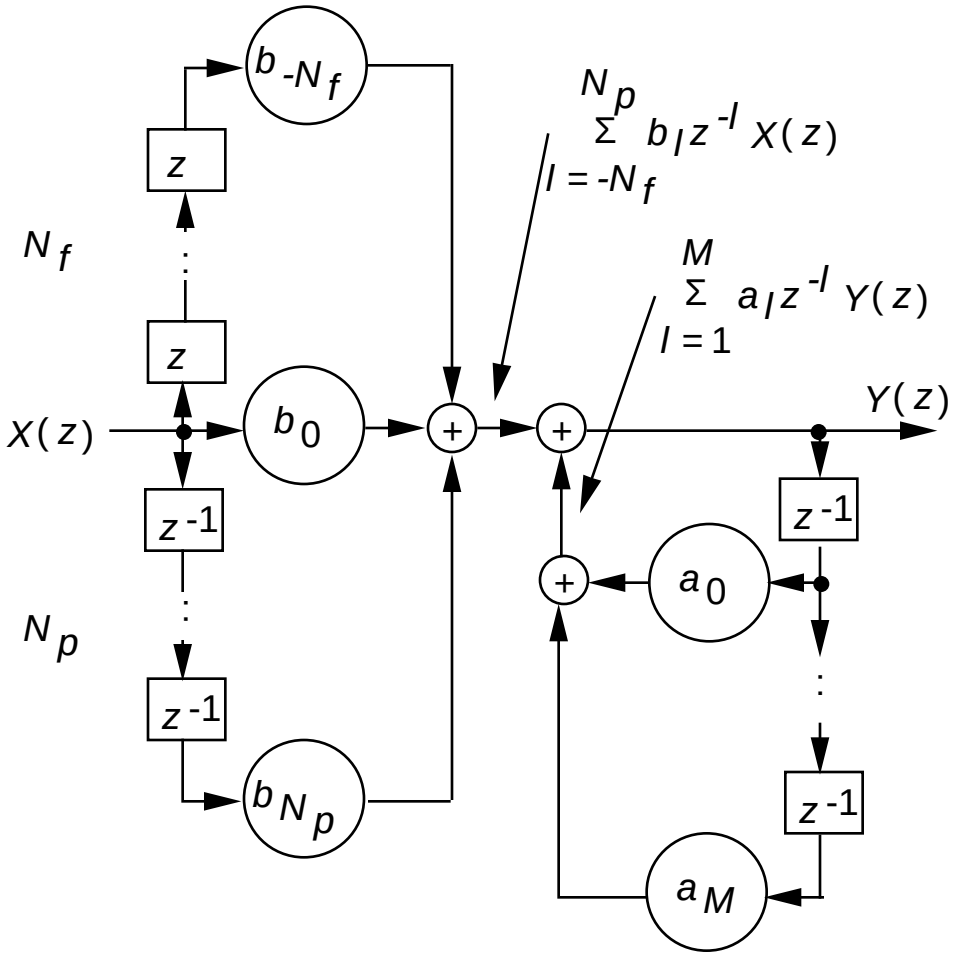
b -Nf
z
Nf
z
X(z)
b0
z -1
Np
z -1
bNp
Np
Σ bl z -l X(z)
l = -Nf
M
Σ al z -l Y(z)
l = 1
Y(z)
z -1
a0
z -1
aM

Figure 1

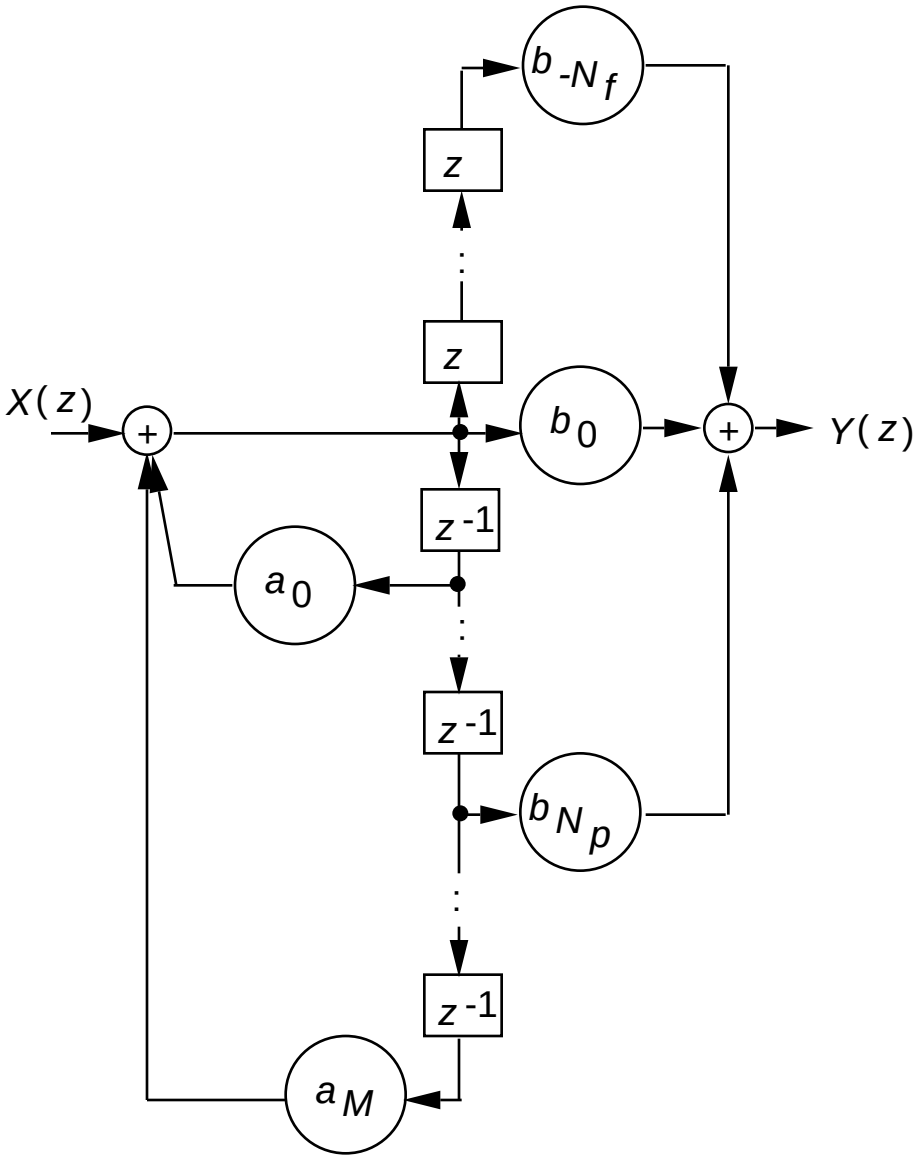

Figure 2

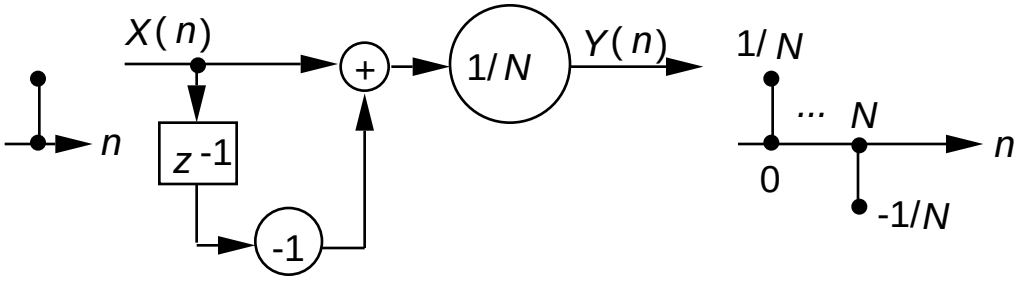

Figure 3

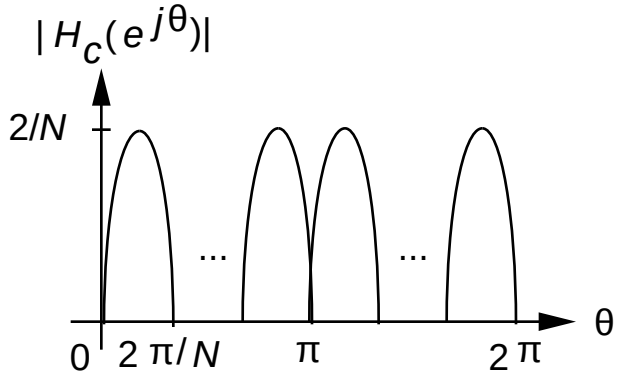

Figure 4

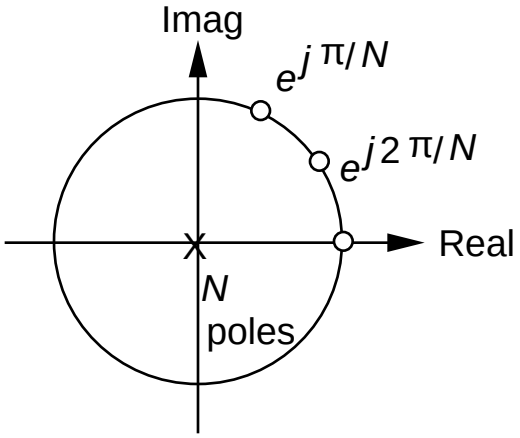

Figure 5

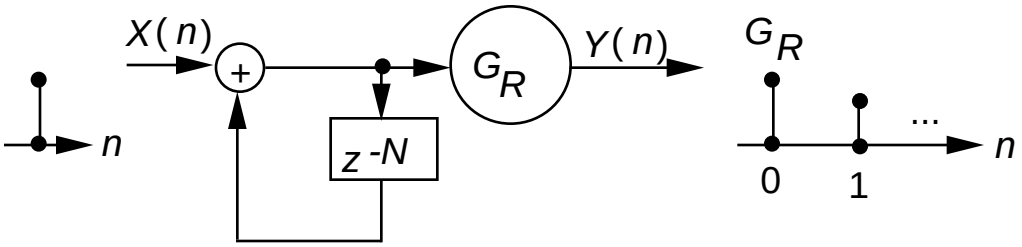

Figure 6

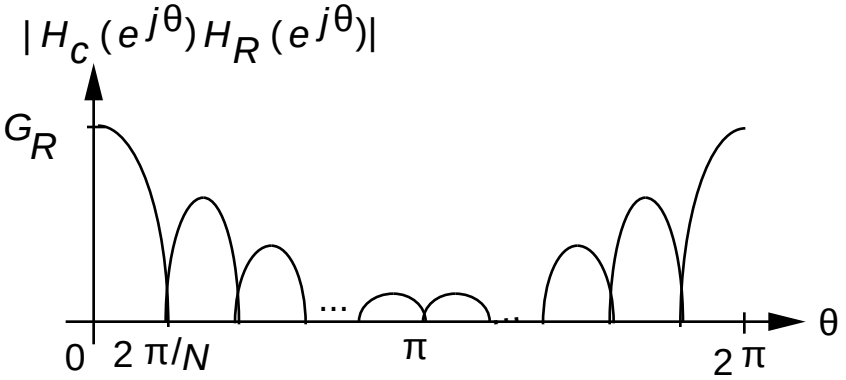

Figure 7

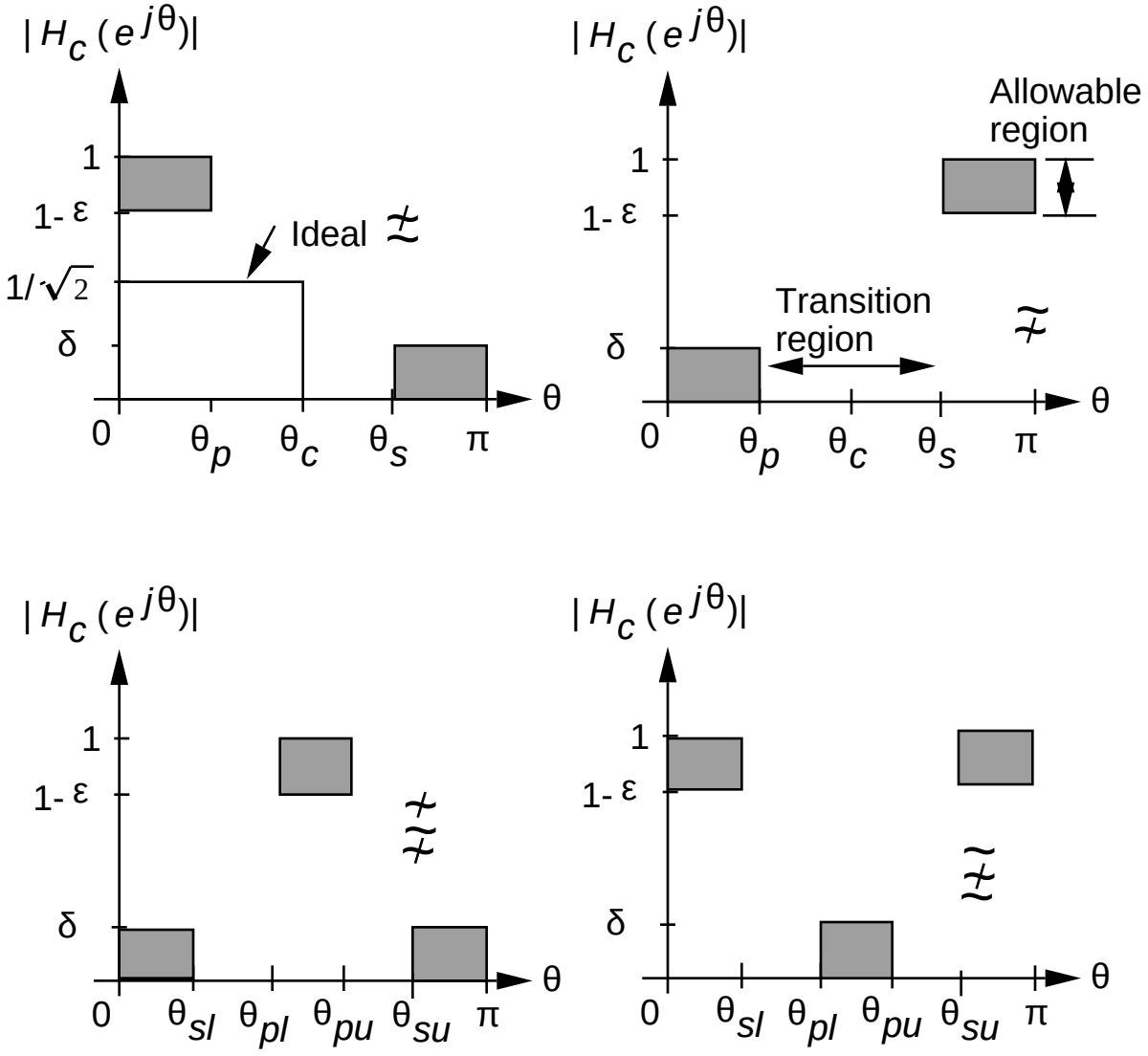
$|H_c(e^{j\theta})|$
1
1- ε
Ideal
$1/\sqrt{2}$
δ
0
θ_p
θ_c
θ_s
π
θ
Allowable region
Transition region
θ_{sl}
θ_{pl}
θ_{pu}
θ_{su}

Figure 8

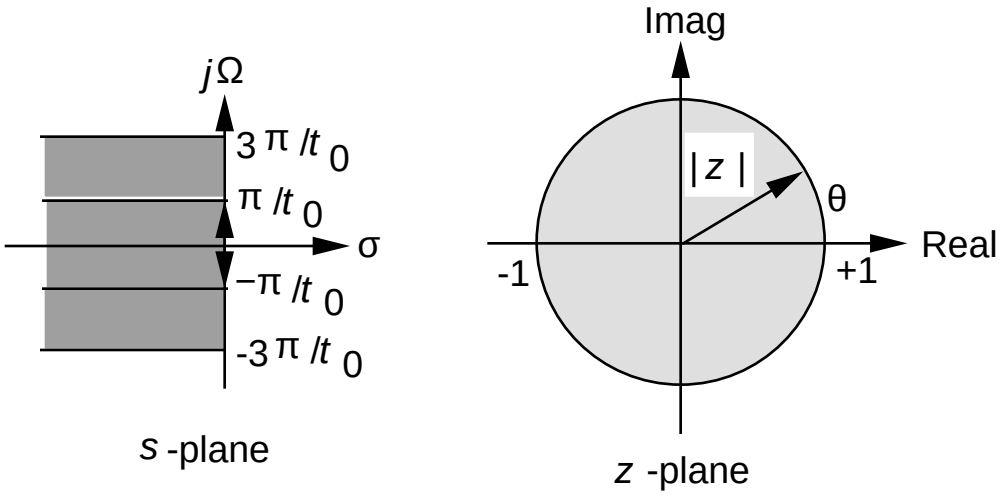

Figure 9

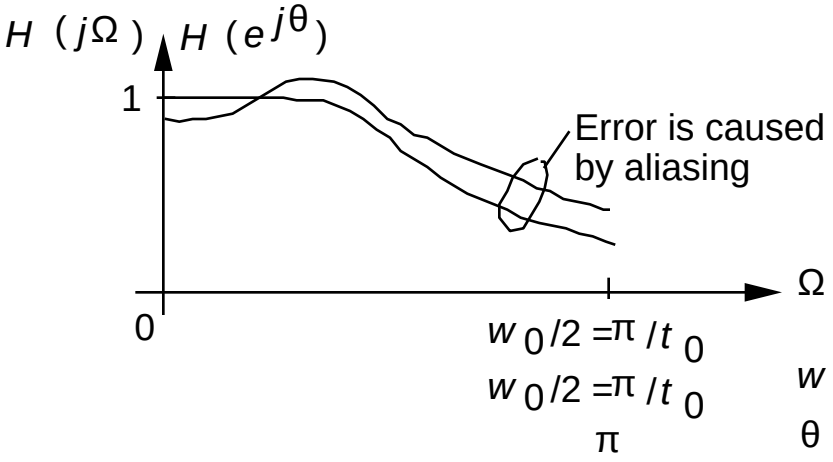

Figure 9.1

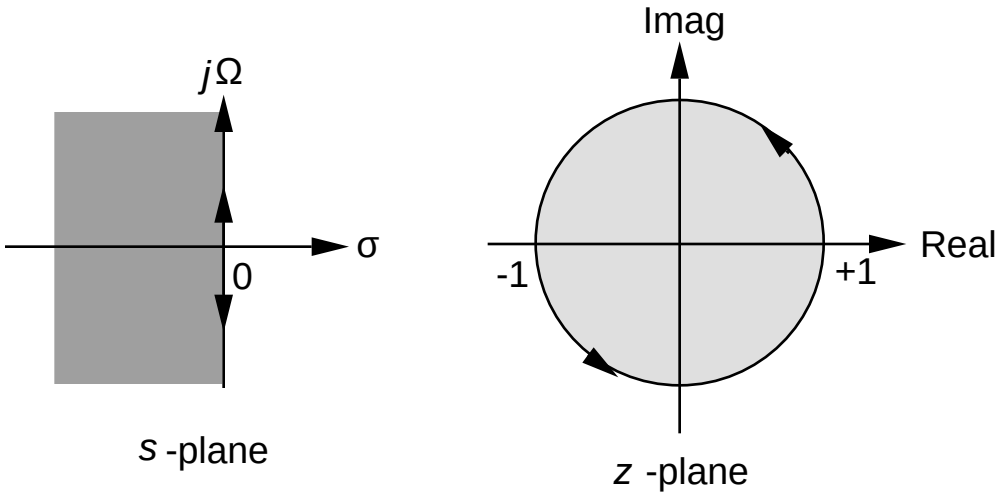

Figure 10

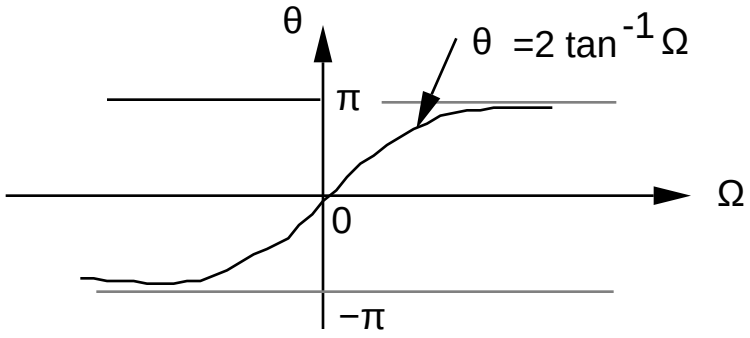

Figure 11

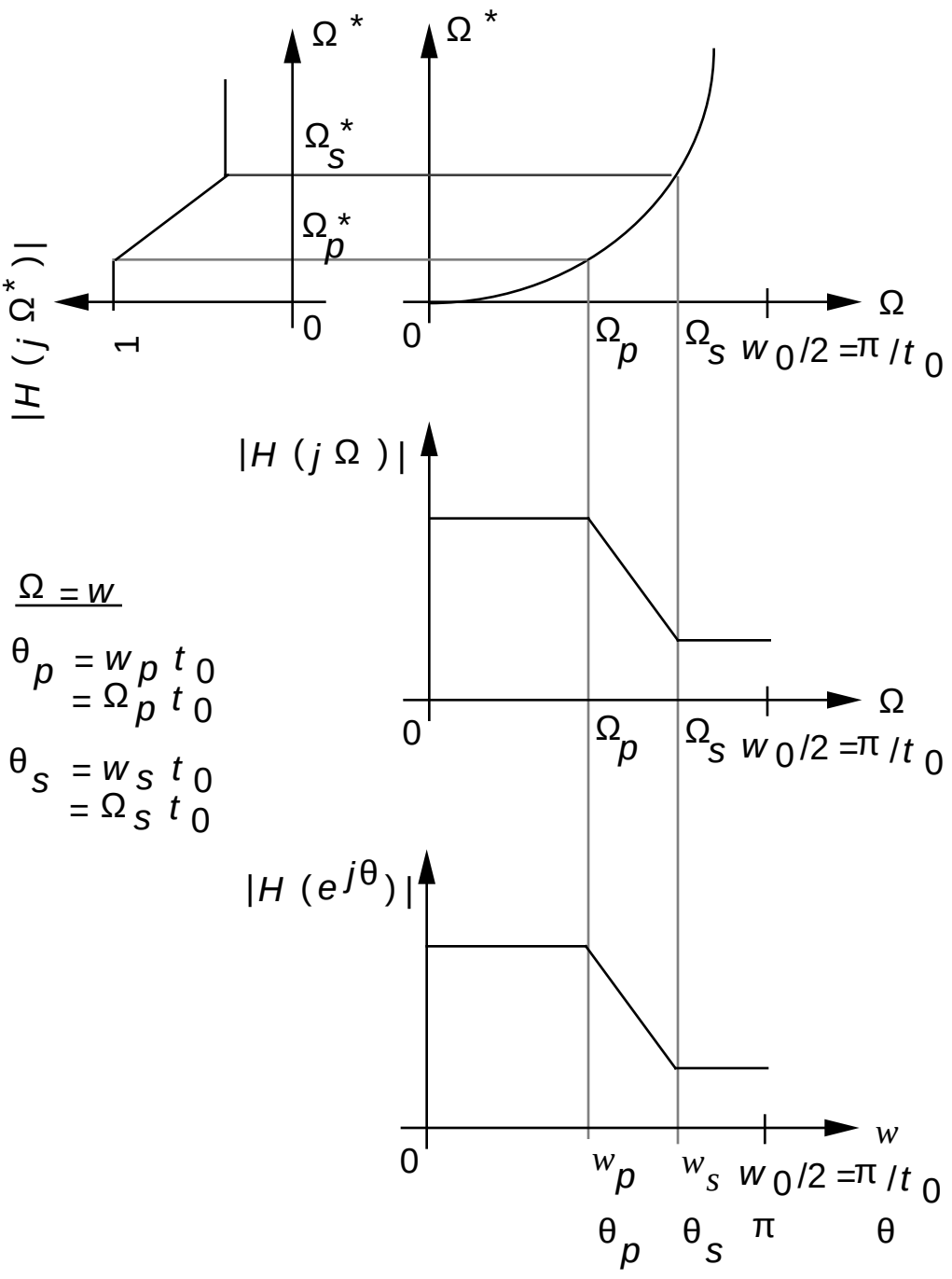
Ω *
Ω *
Ω*s
Ω*p
|H (j Ω*) |
1
0
0
Ω
Ωp
Ωs w0/2 =π /t0
|H (j Ω) |
Ω = w
θp = wp t0
= Ωp t0
θs = ws t0
= Ωs t0
0
Ω
Ωp
Ωs w0/2 =π /t0
|H (e jθ) |
0
w
wp
ws w0/2 =π /t0
θp
θs
π
θ

Figure 12

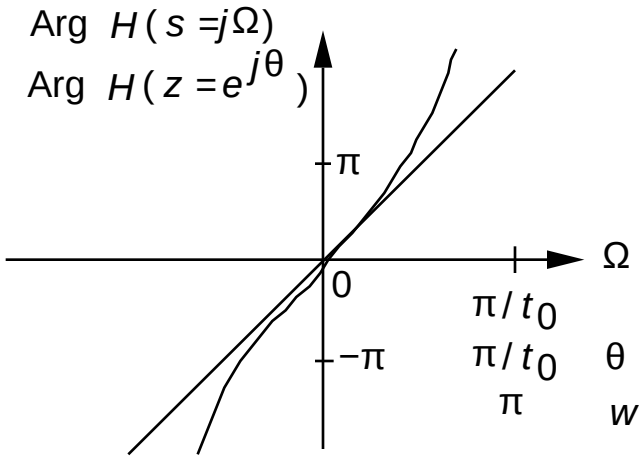

Figure 13

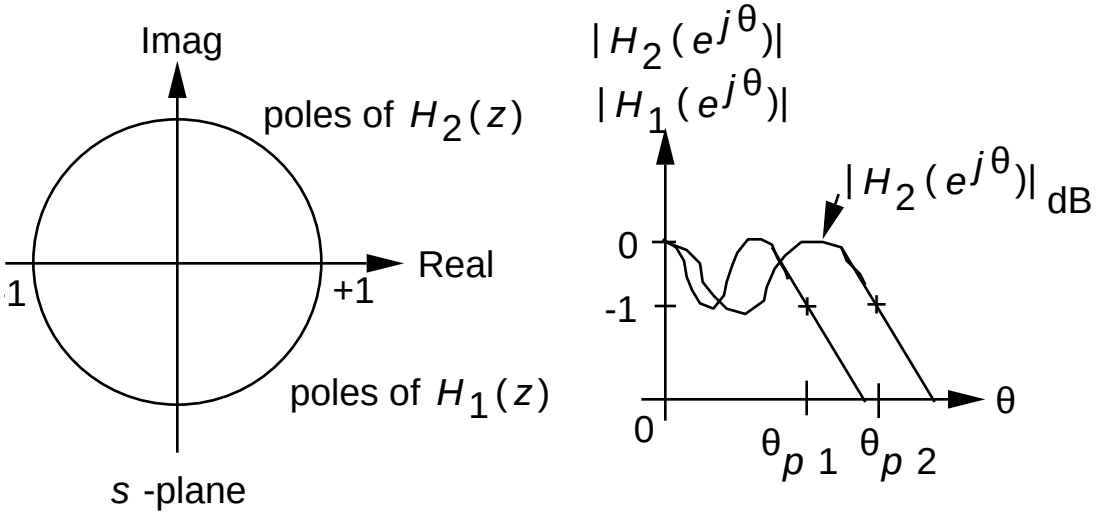

Figure 13.1

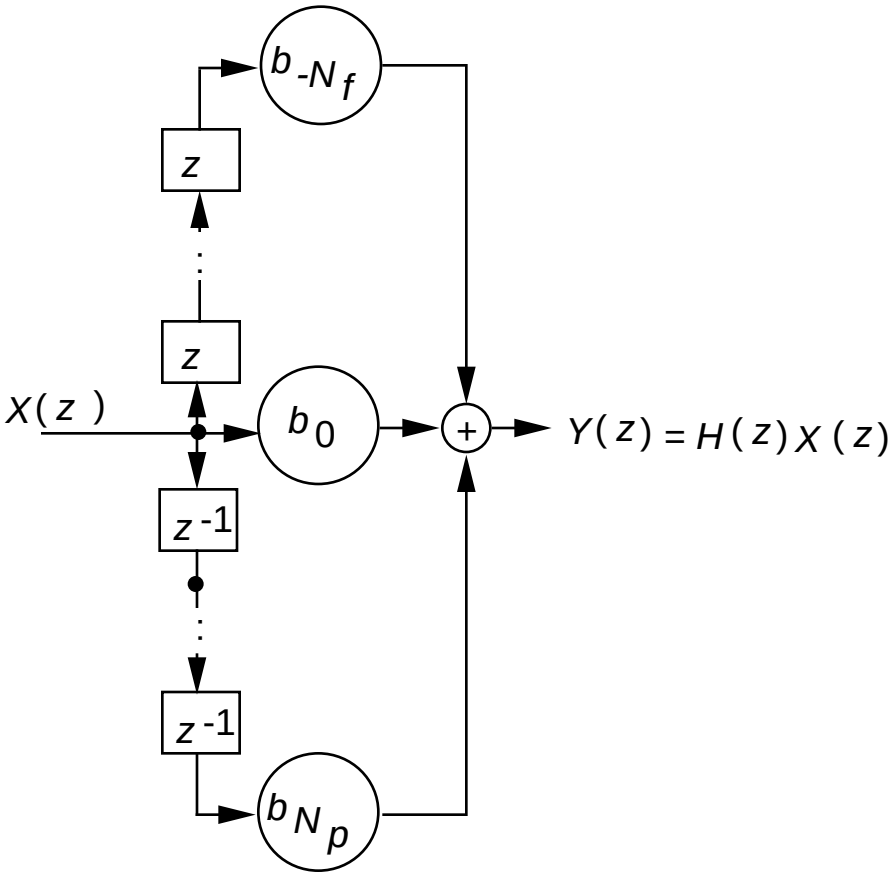

Figure 14

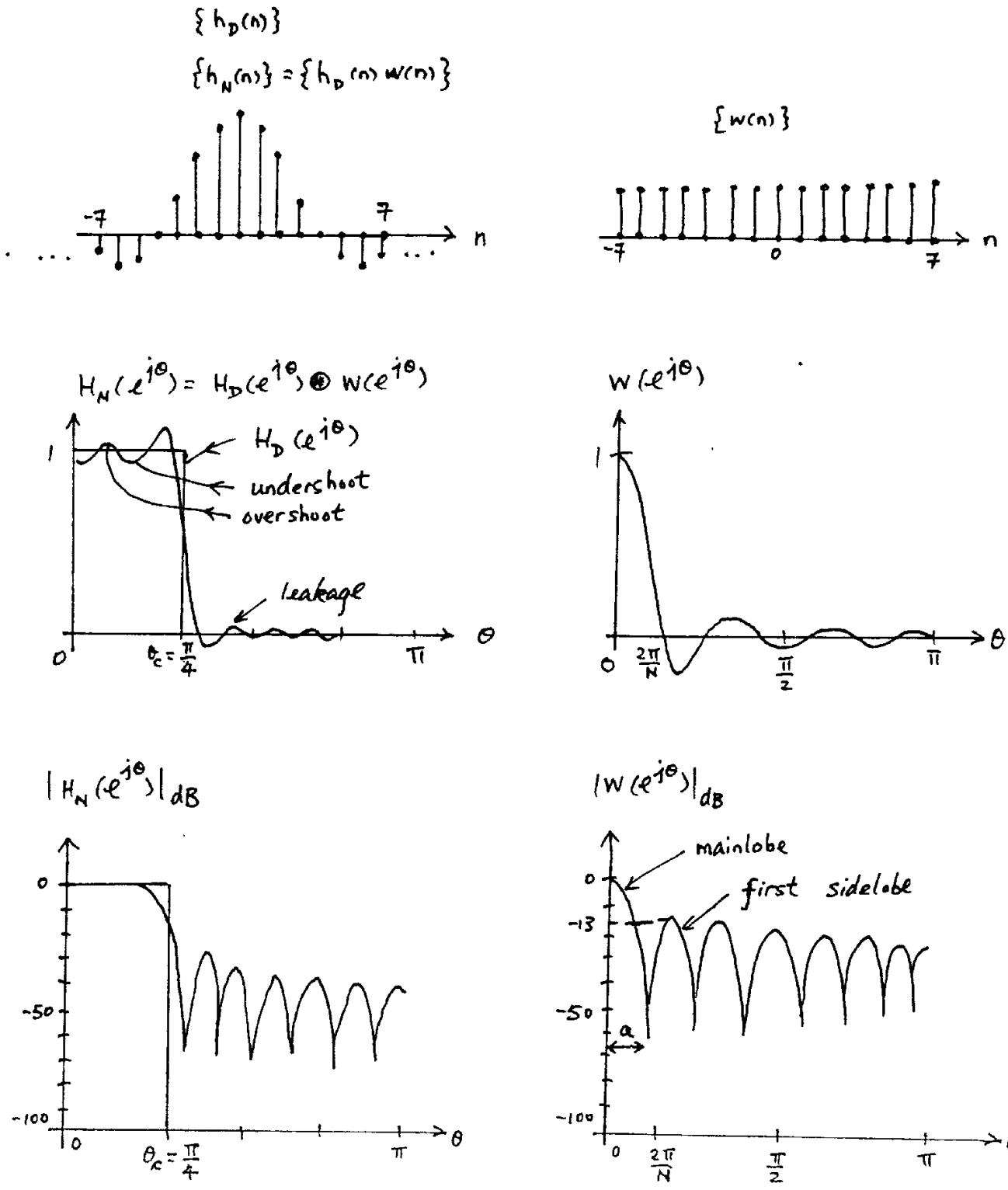
{h_D(n)}
{h_N(n)} = {h_D(n) w(n)}
-7
7
n
{w(n)}
-7
0
7
n
H_N(e^jθ) = H_D(e^jθ) ⊛ W(e^jθ)
H_D(e^jθ)
undershoot
overshoot
leakage
1
0
θ_c = π/4
π
θ
W(e^jθ)
1
0
2π/N
π/2
π
θ
|H_N(e^jθ)|_dB
0
-50
-100
0
θ_c = π/4
π
θ
|W(e^jθ)|_dB
mainlobe
first sidelobe
0
-13
-50
-100
a
0
2π/N
π/2
π
θ

Fig. 15

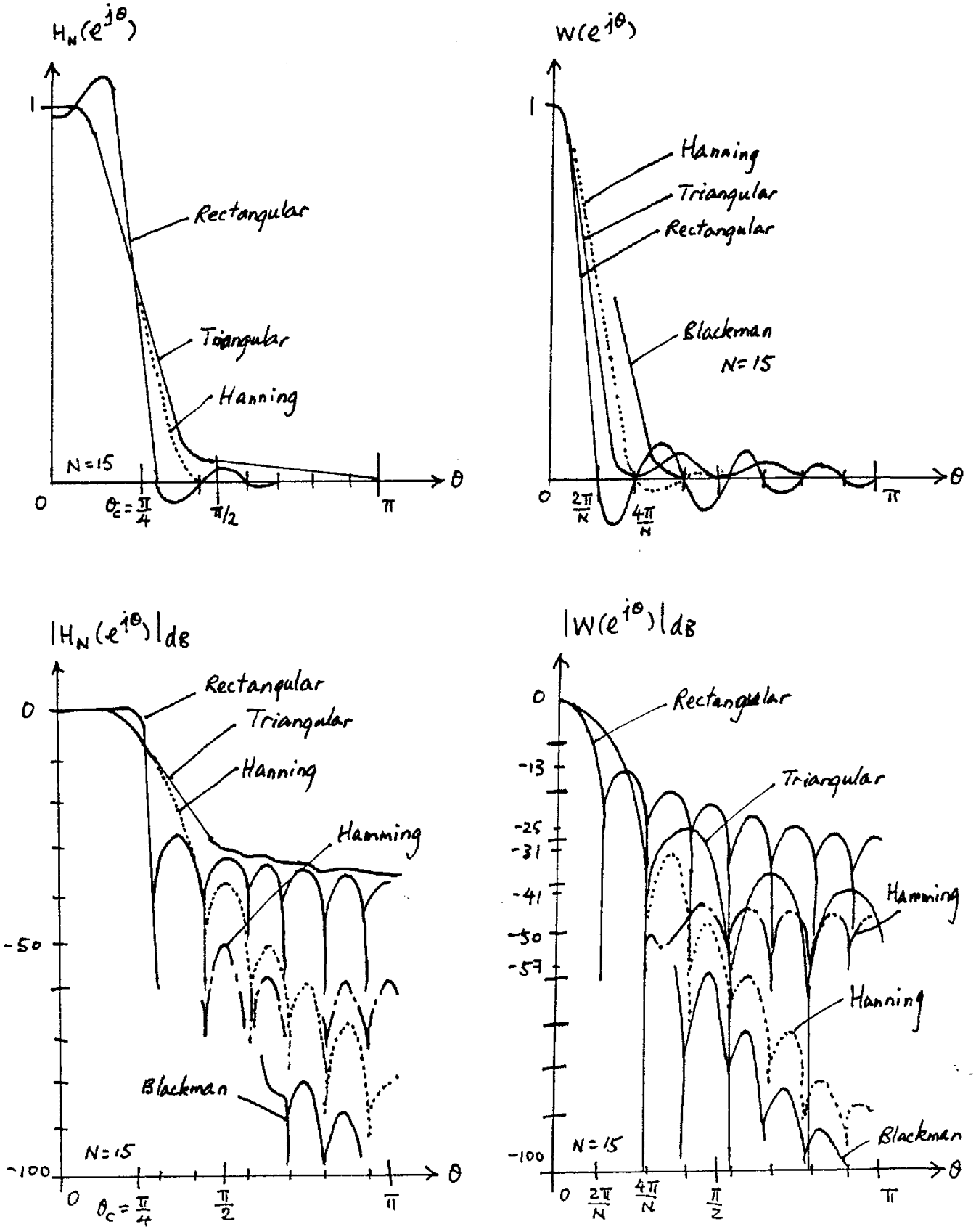
$H_N(e^{j\theta})$
1
Rectangular
Triangular
Hanning
N=15
0
$\theta_c = \frac{\pi}{4}$
$\pi/2$
π
θ
$W(e^{j\theta})$
1
Hanning
Triangular
Rectangular
Blackman
N=15
0
$\frac{2\pi}{N}$
$\frac{4\pi}{N}$
π
θ
$|H_N(e^{j\theta})|_{dB}$
0
-50
-100
Rectangular
Triangular
Hanning
Hamming
Blackman
N=15
0
$\theta_c = \frac{\pi}{4}$
$\frac{\pi}{2}$
π
θ
$|W(e^{j\theta})|_{dB}$
0
-13
-25
-31
-41
-50
-57
-100
Rectangular
Triangular
Hamming
Hanning
Blackman
N=15
0
$\frac{2\pi}{N}$
$\frac{4\pi}{N}$
$\frac{\pi}{2}$
π
θ

Fig. 16

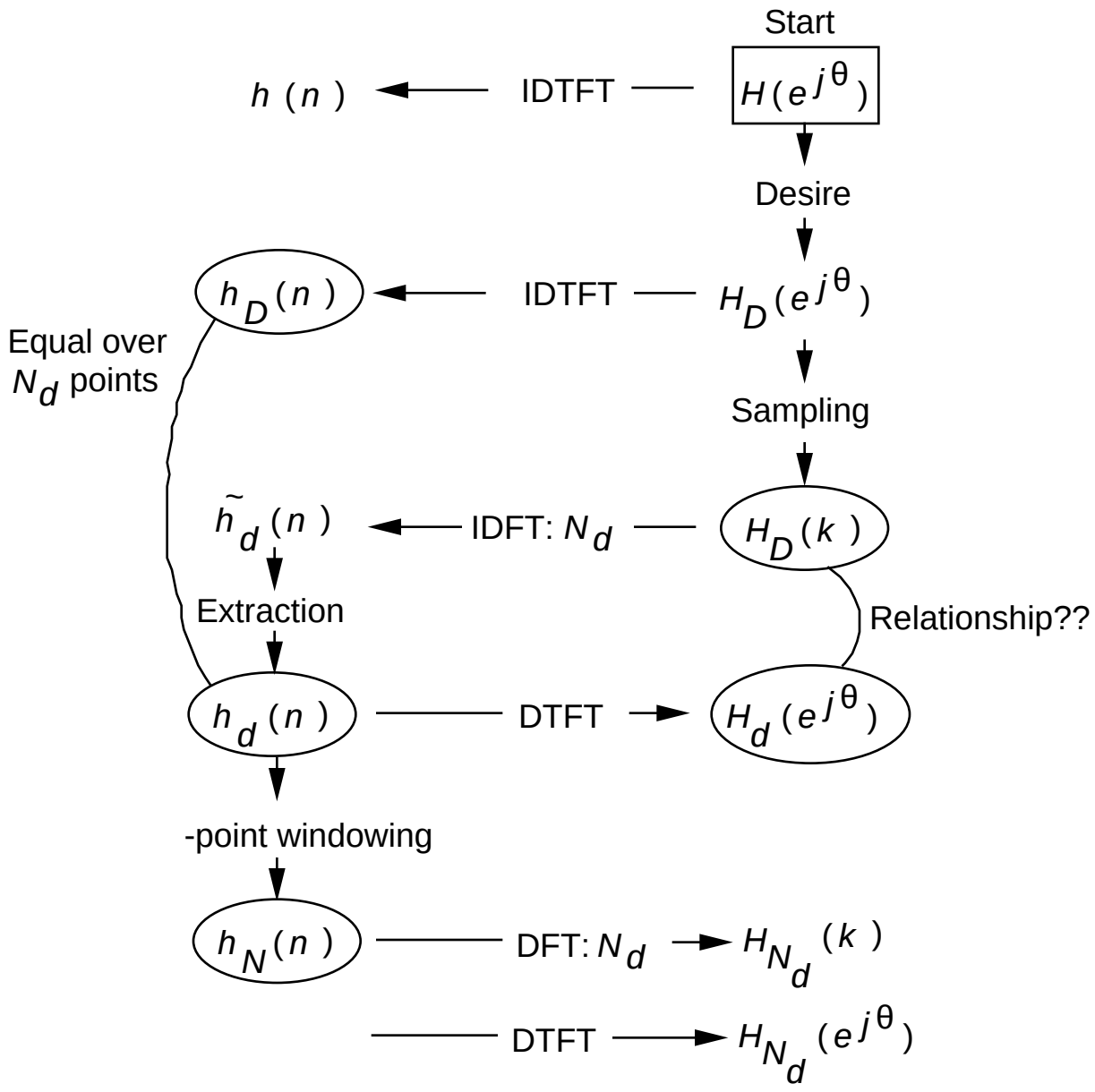
Start
$h(n)$
IDTFT
$H(e^{j\theta})$
Desire
$h_D(n)$
IDTFT
$H_D(e^{j\theta})$
Equal over
N_d points
Sampling
$\tilde{h}_d(n)$
IDFT: N_d
$H_D(k)$
Extraction
Relationship??
$h_d(n)$
DTFT
$H_d(e^{j\theta})$
-point windowing
$h_N(n)$
DFT: N_d
$H_{N_d}(k)$
DTFT
$H_{N_d}(e^{j\theta})$

Figure 17

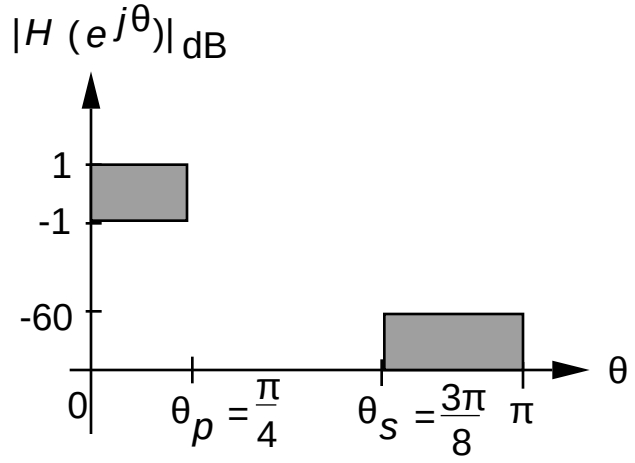

Figure 18

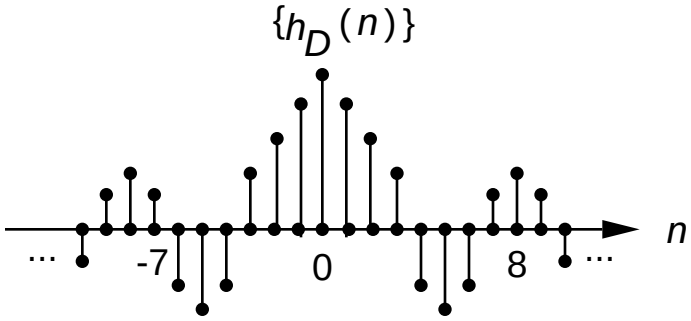

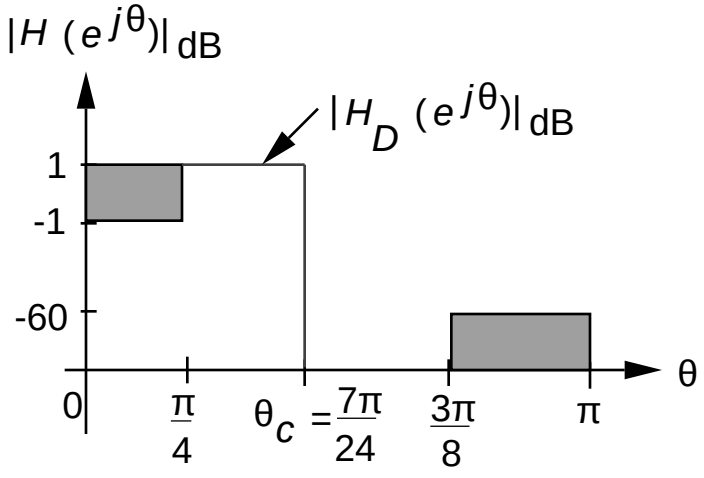

Figure 19

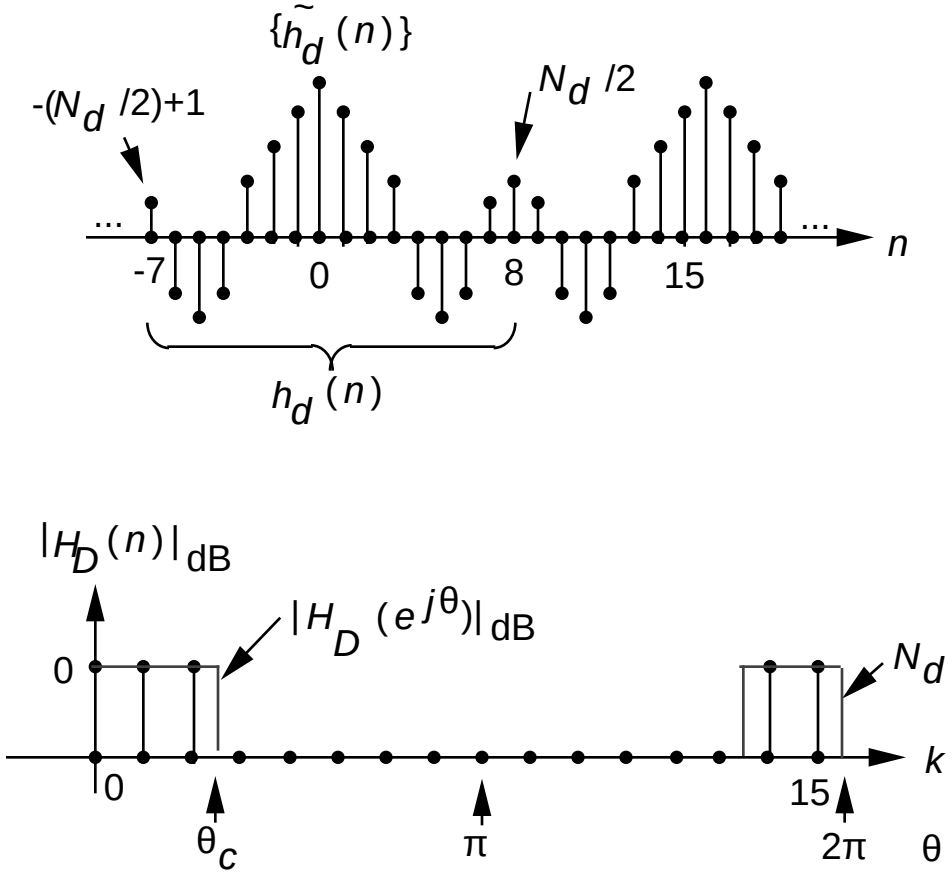
$\{\tilde{h}_d(n)\}$
$-(N_d/2)+1$
$N_d/2$
...
...
n
-7
0
8
15
$h_d(n)$
$|H_D(n)|_{dB}$
$|H_D(e^{j\theta})|_{dB}$
0
N_d
k
0
15
θ_c
π
2π
θ

Figure 20

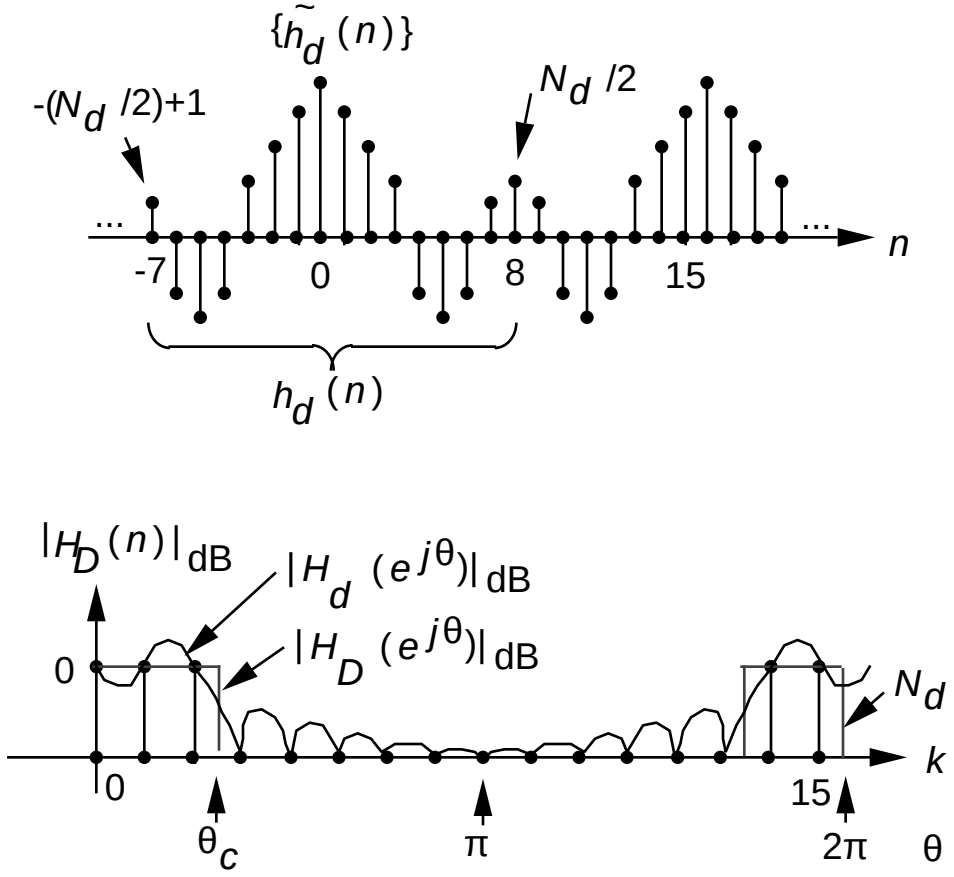
$\{\tilde{h}_d(n)\}$
$-(N_d/2)+1$
$N_d/2$
...
...
n
-7
0
8
15
$h_d(n)$
$|H_D(n)|_{dB}$
$|H_d(e^{j\theta})|_{dB}$
$|H_D(e^{j\theta})|_{dB}$
0
N_d
k
0
15
θ_c
π
2π
θ

Figure 20.1

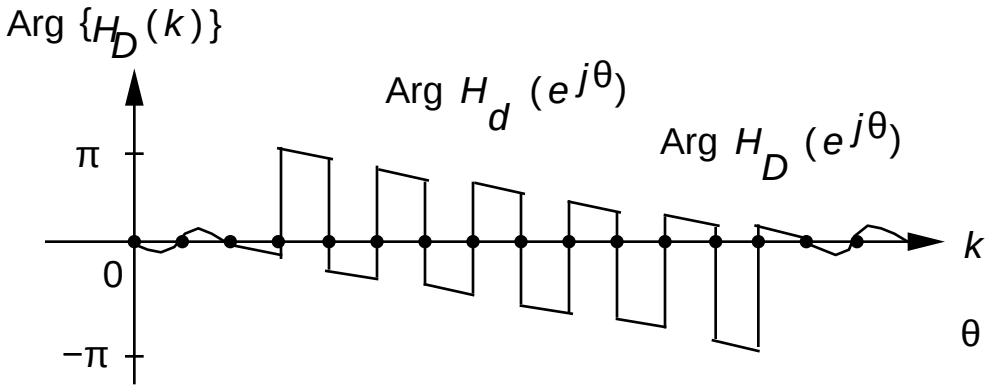

Figure 21

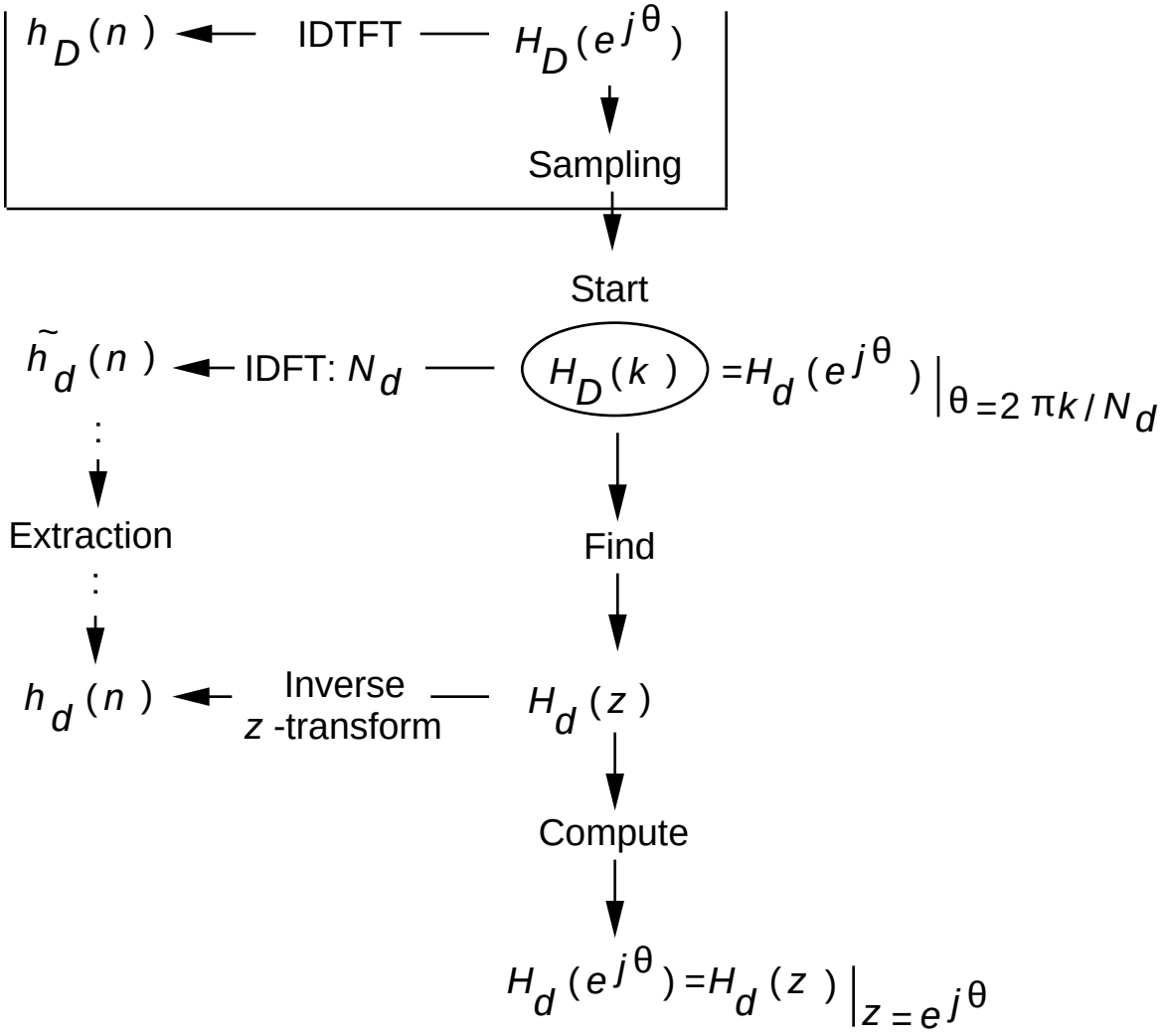

Figure 22

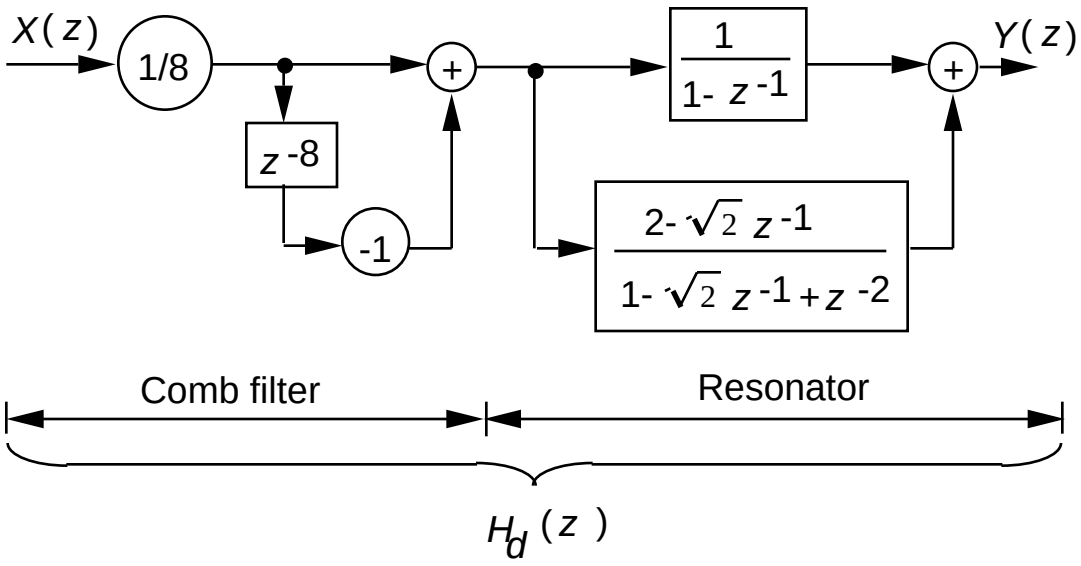

Figure 23

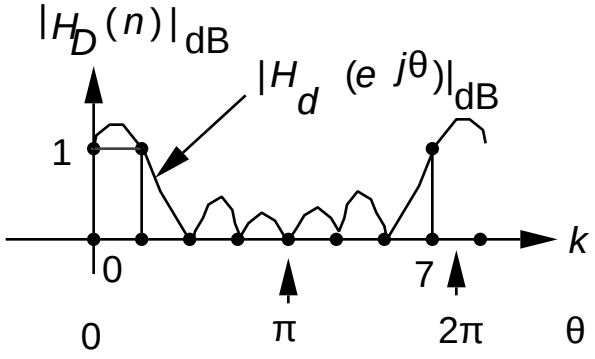

Figure 24